



Cite this: *Chem. Commun.*, 2016, 52, 8645

Received 1st May 2016,  
Accepted 26th May 2016

DOI: 10.1039/c6cc03638d

www.rsc.org/chemcomm

## Halogen bonding anion recognition

Asha Brown\* and Paul D. Beer\*

A halogen bond is an attractive non-covalent interaction between an electrophilic region in a covalently bonded halogen atom and a Lewis base. While these interactions have long been exploited as a tool in crystal engineering their powerful ability to direct supramolecular self-assembly and molecular recognition processes in solution has, until recently, been overlooked. During the last decade however an ever-increasing number of studies on solution-phase halogen-bond-mediated anion recognition processes has emerged. This Feature Article summarises advancements which have been made thus far in this rapidly developing research area. We survey the use of iodoperfluoroarene, haloimidazolium and halotriazole/triazolium halogen-bond-donor motifs in anion receptor design, before providing an account of our research into the application of mechanically interlocked rotaxane and catenane frameworks as halogen bonding anion host systems.

## Introduction

The field of anion recognition has undergone an enormous expansion over recent decades in response to the need to selectively detect, extract and transport negatively charged species, which play fundamental roles in a vast range of chemical, biological, medical and environmental processes.<sup>1,2</sup> However, this area has been appreciably slower to develop than the parallel field of cation coordination chemistry, and the target of producing functional synthetic receptor molecules which emulate the impressive binding affinities and selectivities displayed by natural anion binding proteins<sup>3–6</sup> in aqueous media is still far from realisation. This is commonly attributed to the intrinsic challenges associated with the design of selective host systems for negatively charged species: anions have low charge-to-radius ratios, high solvation enthalpies and poorly defined coordination preferences compared to cations; they are also pH sensitive and exhibit a wide range of geometries. These challenges are often addressed by employing multiple non-covalent interactions in a concerted manner, following well established design principles such as complementarity, chelate cooperativity, preorganisation and the macrocyclic effect. Traditionally, a range of non-covalent interactions including hydrogen-bonding, electrostatic interactions, anion- $\pi$  interactions, dispersion interactions and solvatophobic effects have been used in this way. In particular, hydrogen bonding interactions have been abundantly exploited in both natural and synthetic anion receptors. The halogen bond,<sup>7</sup> which is often described as analogous to the more prevalent hydrogen bond in terms of its comparable binding strengths and directionality, has recently emerged as a powerful alternative non-covalent interaction with immense promise in the

field of anion recognition, yet its importance in this area is still largely unexplored. While halogen bonding interactions have been extensively characterised crystallographically<sup>8–10</sup> and theoretically,<sup>11</sup> and have long been exploited in solid state crystal engineering<sup>12</sup> and materials design applications,<sup>13</sup> it is only during the last 10–15 years that an exploration of the potentially far-reaching solution-phase applications of halogen bonding<sup>14–17</sup> has begun. A recent explosion in the number of studies on halogen bonding interactions in anion coordination and supramolecular chemistry<sup>18</sup> has indicated that these interactions are often complementary to hydrogen bonding in terms of their differing steric requirements, solvent dependencies and anion binding preferences, as well as their inherent tunability; moreover the frequent ability of halogen-bond-based anion receptors to outperform hydrogen-bonding analogues in competitive protic solvent media is becoming increasingly apparent. This Feature Article highlights contributions made by our own group and others to the development of solution-based anion receptors which exploit halogen bonding interactions.

## Fundamentals of halogen bonding

According to the unifying definition proposed by a recent IUPAC Task Group, a halogen bond (XB) “occurs when there is evidence of a net attractive interaction between an electrophilic region associated with a halogen atom in a molecular entity and a nucleophilic region in another, or the same, molecular entity.”<sup>19</sup>

A typical halogen-bonded complex  $R-X \cdots Y$ , where X is the electrophilic XB donor (Lewis acid) and Y the XB acceptor (Lewis base) has several characteristic features: the interatomic  $X \cdots Y$  distance is shorter than the sum of the van der Waals radii of the two interacting atoms; this distance becomes shorter as the strength of the XB interaction increases; a concomitant up to 0.03 Å increase in the length of the covalent

Chemical Research Laboratory, Department of Chemistry, University of Oxford, Mansfield Road, Oxford, OX1 3TA, UK. E-mail: paul.beer@chem.ox.ac.uk

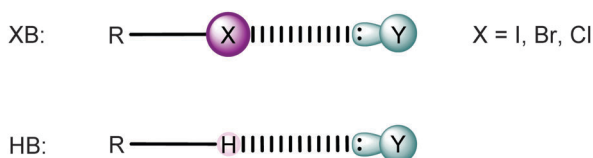


Fig. 1 Schematic comparison of halogen-bonding (XB) and hydrogen-bonding (HB) interactions.

R–X bond compared to that in the non-halogen-bonded complex is observed; the R–X...B angle is close to  $180^\circ$ ;<sup>10,20,21</sup> the interaction strength lies within the range  $10\text{--}200\text{ kJ mol}^{-1}$ ,<sup>22,23</sup> which is broadly similar to the range spanned by hydrogen-bonding (HB) interactions. The term ‘halogen bond’ was originally conceived in recognition of the geometric and energetic parallels between XB and HB interactions (Fig. 1).<sup>24,25</sup> However, there are also important differences between the two classes of interaction; for example XB interactions have a more stringent preference for linearity than HB interactions,<sup>26</sup> are typically more hydrophobic in character and exhibit different solvent dependencies.<sup>27</sup>

The apparent paradox of electronegative halogen atoms functioning as electrophilic species can be understood in terms of the anisotropic distribution of electron density around a covalently bonded halogen atom. The calculated molecular electrostatic potential surfaces of molecules incorporating halogen atoms are characterised by a localised region of depleted electron density along the extension of the R–X bond axis, termed a ‘ $\sigma$ -hole’ (Fig. 2).<sup>29</sup> This electron deficient region is immediately surrounded by an electroneutral region, followed by a lateral belt of negative electrostatic potential, which accounts for the amphoteric ability of halogen atoms to also interact attractively with electrophiles approaching orthogonally to the covalent R–X bond. The highly localised nature of the  $\sigma$ -hole justifies the strictly linear nature of XB interactions; its size—and hence the strength of the observed XB interaction—generally increases with decreasing electronegativity and increasing polarisability of the halogen atom X ( $\text{I} > \text{Br} > \text{Cl} \gg \text{F}$ ),<sup>30,31</sup> and with increasing electron-withdrawing ability of the substituent R. While this electrostatic  $\sigma$ -hole model accounts for most experimentally observed features of XB interactions, there are arguably some anomalies for which additional contributions from charge-transfer and dispersion

components have been proposed to give a satisfactory explanation. A large number of theoretical and experimental studies have sought to elucidate the various contributions to the observed interactions;<sup>32</sup> however, there is still heated debate about the classification of XB interactions and it is probable that the relative importance of the various electrostatic/polarisation, charge transfer and dispersion contributions vary from system to system, depending on the local environment and nature of the interacting partners.<sup>†</sup>

## Halogen bonding in anion recognition

Anions are by nature electron-rich and can therefore be predicted to give rise to strong attractive interactions when acting as XB acceptors.<sup>33,34</sup> This proposition has instigated a flurry of interest in the incorporation of XB donor groups into anion receptor molecules in recent years. The vast majority of the receptors developed to date have incorporated haloperfluoroarene, halotriazole/halotriazolium or haloimidazolium motifs as polarised XB donor groups (Fig. 3a), which have generally been employed in a multivalent manner, either alone or in cooperation with other non-covalent interactions such as hydrogen-bonding. The following sections survey the use of each of these motifs in anion receptor design, before detailing our own attempts to exploit the interior cavities of mechanically bonded rotaxane and catenane architectures as three-dimensional scaffolds on which to append XB donor groups, in order to facilitate complete encapsulation of the guest anion within the shielded microenvironment of the host’s interlocked binding domain (Fig. 3b).

### Haloperfluoroarene halogen bond donor groups

The potential of XB interactions to direct anion recognition processes in solution was first demonstrated in a seminal 2005 publication by Metrangolo, Resnati and co-workers.<sup>35</sup> A heteroditopic receptor (**1a**, Fig. 4) incorporating tris(polyoxyethylene)amine and 4-iodotetrafluorophenyl recognition sites for a cation and counteranion respectively was shown *via*  $^1\text{H}$  NMR competition experiments to complex a separated NaI ion-pair with significantly higher affinity than the analogous perfluorinated monotopic receptor **1b** ( $K_{1a} = 2.6 \times 10^5\text{ M}^{-1}$ ;  $K_{1b} = 1.3 \times 10^4\text{ M}^{-1}$ ) in  $\text{CDCl}_3$ . Mass spectrometry competition experiments demonstrated the XB receptor’s ability to selectively complex  $\text{I}^-$  in the presence of  $\text{Cl}^-$  and  $\text{Br}^-$  anions. Solid state characterisation of the NaI complex of **1a** confirmed the existence of C–I... $\text{I}^-$  halogen bonds between the pendant iodoperfluoroaryl groups and the iodide anion. However, owing to the divergent arrangement of the halogen bond donor groups the anion is unable to

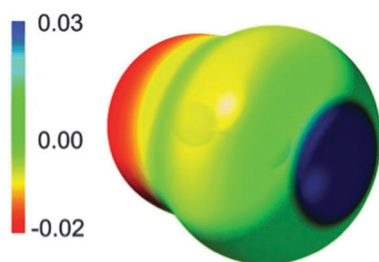
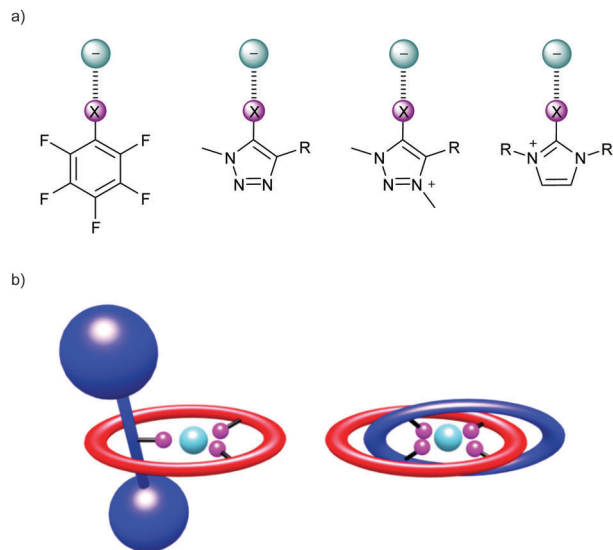
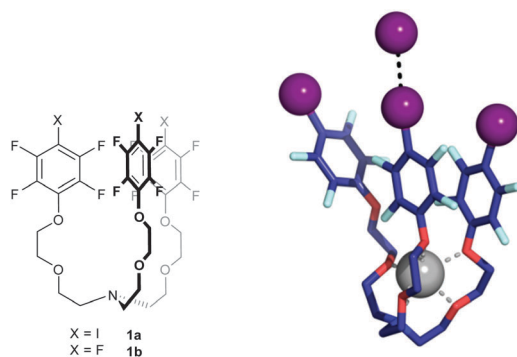


Fig. 2 Calculated molecular electrostatic potential of BrF mapped on the molecular surface (isosurface of 0.001 a.u.) showing the anisotropic distribution of charge around the bromine atom, and the  $\sigma$ -hole. Scale in atomic units. Adapted from ref. 28 with permission from the PCCP Owner Societies.

<sup>†</sup> In addition, several authors have questioned the validity of attempting to decompose the binding energy into discrete contributions, emphasising that all interatomic interactions are fundamentally electrostatic in nature and that, while the electrostatic/polarisation and charge transfer/covalency classifications are conceptually useful aids in understanding the nature of halogen bonding, they are not truly independent or physically distinct: each represents a mathematically constructed model to rationalise the measured binding energy, which is the only physically observable quantity, and as such the difference between them is largely one of semantics.<sup>11,97,98</sup>



**Fig. 3** (a) Examples of XB-donating haloperfluoroarene, halotriazole, halotriazolium and haloimidazolium motifs commonly used in anion recognition. (b) Schematic representation of interlocked [2]rotaxane (left) and [2]catenane (right) anion host systems incorporating multiple convergent XB donor groups.



**Fig. 4** Chemical structure of Resnati and Metrangolo's heteroditopic halogen-bonding ion-pair receptor **1a**, and solid state structure of the **1a**·NaI complex. Hydrogen atoms have been omitted for clarity. I...I<sup>−</sup> halogen-bonding interaction represented as black dashed line.

interact with the receptor's three XB donor groups in a cooperative manner and a monodentate *exo*-binding mode is instead observed, with each iodide anion forming bridging XBs to adjacent molecules in an infinite linear chain.

Subsequently Taylor and co-workers reported a series of monodentate, bidentate and tridentate iodoperfluoroarene derivatives capable of recognising anions solely *via* single or multiple convergent halogen-bonding interactions in acetone solution.<sup>36–38, 19</sup> <sup>19</sup>F NMR titration experiments demonstrated that the tripodal receptor **2a** (Fig. 5a) binds halide anions with the highest affinities in acetone-d<sub>6</sub>, with Cl<sup>−</sup> ( $K = 1.9 \times 10^4 \text{ M}^{-1}$ ) being bound selectively over Br<sup>−</sup> and I<sup>−</sup>.<sup>36</sup> van't Hoff analysis revealed that Cl<sup>−</sup> recognition is driven by favourable enthalpic ( $\Delta H_{\text{binding}} = -3.9 \text{ kcal mol}^{-1}$ ) and entropic ( $\Delta S_{\text{binding}} = +6.1 \text{ kcal mol}^{-1}$ ) terms, while a series of control experiments demonstrated that the analogous receptors **2b–d**, in which the

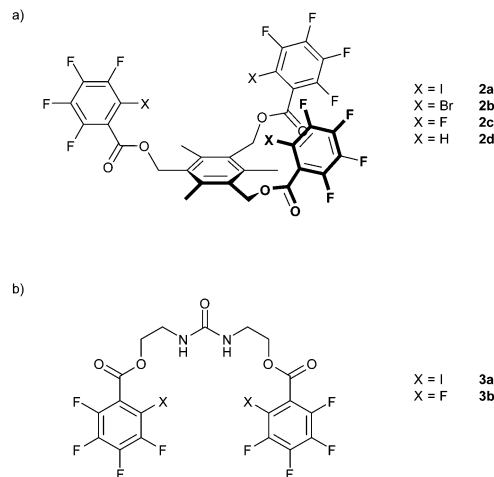


**Fig. 5** Taylor's haloperfluoroarene-based XB anion receptors: (a) tripodal all halogen-bonding systems and corresponding perfluorinated and C–H substituted controls systems and (b) a hybrid receptor employing four convergent C–I and N–H halogen- and hydrogen-bond-donor groups (**3a**) and corresponding perfluorinated control system (**3b**).

iodine atom is replaced by bromine, fluorine and hydrogen atoms respectively, displayed comparatively modest ( $K < 10 \text{ M}^{-1}$ ) chloride binding affinities. In contrast to geometrically similar tridentate HB receptors,<sup>39,40</sup> compound **2a** did not show a measureable affinity for the oxoanions TsO<sup>−</sup>, HSO<sub>4</sub><sup>−</sup> and NO<sub>3</sub><sup>−</sup>, suggesting an innate preference of the XB donor groups for softer halide over harder oxoanion acceptors, possibly as a consequence of significant charge transfer and/or dispersion contributions to the C–I...A<sup>−</sup> XB interaction. Huber, Keller *et al.* described a detailed analysis of the solid state structures, calculated gas phase structures and solution phase anion binding properties of bi- and tridentate fluorinated iodo-benzene derivatives, including an interesting study on the solvent dependencies of the receptors' halide binding affinities.<sup>41</sup> The Taylor group have also described the anion recognition properties of a series of mixed hydrogen- and halogen-bonding receptors equipped with a bidentate urea HB-donor group in addition to either one or two iodoperfluorobenzoate halogen-bond-donor groups. Comparison of these receptors with control systems which lack the iodine XB donor substituent revealed that the presence of the XB donor groups selectively amplifies the receptors' affinities for halide anions (estimated incremental free energy per halogen bond,  $\Delta\Delta G_{\text{XB}} \leq 1.1 \text{ kcal mol}^{-1}$ ) compared to NO<sub>3</sub><sup>−</sup>, HSO<sub>4</sub><sup>−</sup>, H<sub>2</sub>PO<sub>4</sub><sup>−</sup>, TsO<sup>−</sup> and BzO<sup>−</sup> oxoanions ( $\Delta\Delta G_{\text{XB}} \leq 0.4 \text{ kcal mol}^{-1}$ ).<sup>42</sup> The XB receptors were shown to recognise halides with binding constant in the range  $1.1 \times 10^2 \leq K \leq 2.1 \times 10^4 \text{ M}^{-1}$  in acetonitrile-d<sub>3</sub> with the general selectivity trend Cl<sup>−</sup> > Br<sup>−</sup> > I<sup>−</sup>. The most significant XB enhancement effect was displayed by the symmetric bis-iodoperfluorobenzoate-functionalised receptor **3a** (Fig. 5b), whose halide association constants are 16–30 times higher than those of the perfluorinated control receptor **3b**.

Feng and co-workers have described a dendritic organogelator molecule functionalised with peripheral iodoperfluorophenyl XB donor groups which operates as a specific visual sensor for Cl<sup>−</sup> anions.<sup>43</sup> In the absence of Cl<sup>−</sup> anions the dendritic organogelator **4** (Fig. 6a) was shown to form stable gels in a range of

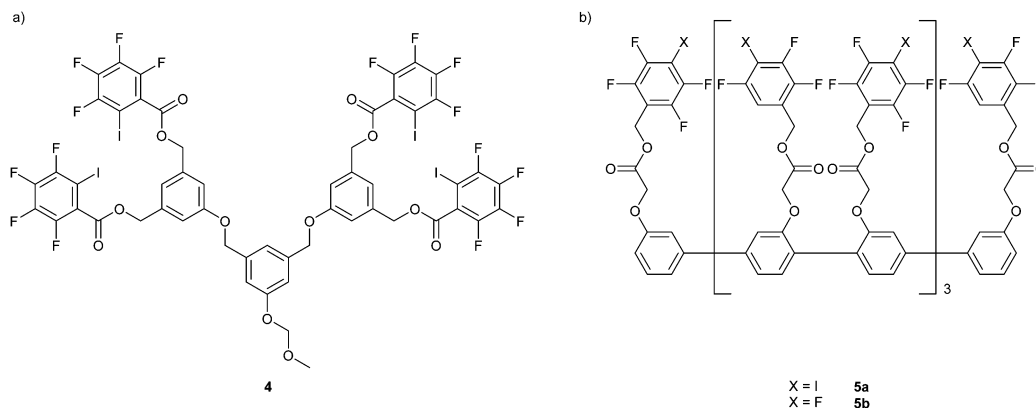


Fig. 6 Functional iodoperfluoroaryl systems exploiting C–I...anion interactions: (a) Feng's chloride-responsive organogelator and (b) Matile's transmembrane XB cascades.

organic solvents. The addition of TBACl triggered a sol–gel phase transition, causing complete collapse of the gel within 10 minutes. This effect was attributed to a perturbation in the conformation of the organogelator molecules as a result of XB interactions between the  $\text{Cl}^-$  anion and iodophenyl XB donor groups, which in turn disrupt the aromatic stacking interactions which drive the gelation process. In contrast other anions such as  $\text{Br}^-$ ,  $\text{I}^-$ ,  $\text{NO}_3^-$ ,  $\text{HSO}_4^-$  and  $\text{CN}^-$  were found to induce only partial or negligible collapse of the gel, even when present in excess. Matile and co-workers have investigated the incorporation of iodoperfluorophenyl XB donor groups into synthetic anion transporter molecules which take advantage of the strength, directionality and intrinsically hydrophobic nature of XB interactions.<sup>44–46</sup> The linear XB octameric derivative **5a** (Fig. 6b) was shown to effect  $\text{Cl}^-/\text{OH}^-$  antiport across a lipid bilayer membrane with an  $\text{EC}_{50}$  value of  $0.11 \pm 0.02 \mu\text{M}$ , the highest anion transport activity reported for a XB transporter reported to date.<sup>46</sup> In contrast, the non-halogenated control receptor **5b** is 26 times less active ( $\text{EC}_{50} = 2.9 \pm 0.4 \mu\text{M}$ ).<sup>46</sup>

### Haloimidazolium halogen bond donor groups

Having formerly exploited imidazolium derivatives as charge-assisted C–H hydrogen bond donors in anion recognition processes,<sup>47–50</sup> we recently became interested in investigating the analogous XB-driven anion recognition capabilities of 2-haloimidazolium derivatives. X-ray structural analysis of the hexyl- and benzyl-substituted haloimidazolium salts **6-Br** and **7a-Br** and **7b-A** ( $\text{A} = \text{Cl}^-$ ,  $\text{I}^-$ ; Fig. 7a) provided a preliminary indication of the capability of these motifs to form strong, linear halogen bonds with halide counteranions (Table 1).<sup>51,52</sup> Similarly Resnati, Metrangolo and co-workers characterised the solid state  $\text{Cl}^-$ ,  $\text{Br}^-$  and  $\text{I}^-$  complexes of a 2-iodoimidazolium receptor (**8a**) bearing an anthracenyl substituent (Fig. 7b), observing strong, linear XB interactions for all three halide complexes.<sup>53</sup> Interestingly, a surprisingly short I–O XB interaction was observed in the crystal structure of the  $\text{H}_2\text{PO}_4^-$  complex of this receptor (Table 1). Furthermore solution  $^1\text{H}$  NMR studies showed that compound **8a-I** is able to bind  $\text{H}_2\text{PO}_4^-$  ( $K_{11} = 1100 \pm 300$ ) selectively over  $\text{AcO}^-$ ,  $\text{Cl}^-$ ,  $\text{Br}^-$  and  $\text{I}^-$  anions in DMSO solution, which constitutes a rare example of an oxoanion-selective

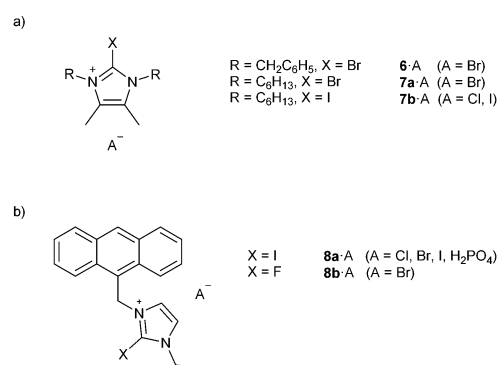


Fig. 7 Monodentate haloimidazolium anion receptors molecules: (a) Beer's 4,5-dimethyl-substituted bromoimidazolium and iodoimidazolium derivatives and (b) Resnati and Metrangolo's anthracenyl-appended variant.

XB-driven anion recognition process. In the polar, aprotic DMSO solvent medium the halide anions are bound in order of increasing charge density ( $\text{Cl}^- > \text{Br}^- > \text{I}^-$ ), and a marginal preference for  $\text{AcO}^-$  over  $\text{Cl}^-$  is observed.<sup>‡</sup> It is also noteworthy that the anion binding affinities of the XB receptor **8a-I** surpass those of the corresponding HB receptor **8b-I** for all anions studied. A recent theoretical study by Lu *et al.* provides further insight into the degree of electrostatic, dispersion and covalent contributions to the XB interactions in such haloimidazolium-based anion receptors.<sup>54</sup>

With the aim of enhancing the anion binding affinities and selectivities of the acyclic monodentate haloimidazolium receptors described above we developed a series of macrocyclic haloimidazoliophane receptors which are capable of recognising halide anions in a competitive aqueous methanolic solvent mixture solely *via* charge assisted bidentate XB interactions.<sup>56–59</sup>

‡ When interpreting this trend, and in particular the association constant obtained for iodide, it should be taken into account that the  $^1\text{H}$  NMR titration protocol which was used to determine association constants involved titration of TBA salts of the various anions into the iodide salt of the receptor. Despite the presence of the iodide counteranion, the authors state that a semi-quantitative comparison of the iodide association constant remains valid because the receptor's affinity for iodide is low.



**Table 1** Details of XB distances and angles in the solid state structures of compounds **6-Br**, **7-A** and **8a-A**<sup>51–53</sup>

	<b>6-Br</b>	<b>7a-Br<sup>b</sup></b>	<b>7b-Cl</b>	<b>7b-I</b>	<b>8a-Cl</b>	<b>8a-Br</b>	<b>8a-I</b>	<b>8a-H<sub>2</sub>PO<sub>4</sub><sup>c</sup></b>
X...A <sup>−</sup> (Å)	3.297	3.159(0) 3.158(0)	2.948(1)	3.289(0)	3.023(1)	3.099(1)	3.283(1)	2.602(2)
R <sub>XA</sub> <sup>a</sup>	89	85 85	79	83	81	81	83	74
C-X (Å)	1.859(2)	1.860(4) 1.860(4)	2.092(5)	2.117(4)	2.081(2)	2.093(3)	2.086(6)	2.095(3)
C-X...A <sup>−</sup> angle (°)	172.6	168.1(1) 168.2(1)	177.6(1)	177.6(1)	174.1(1)	178.5(1)	171.9(2)	177.8(2)

<sup>a</sup>  $R_{XA} = d(XA)/(r_X + r_A)$  where  $r_X$  and  $r_A$  refer to the van der Waals radii of the 2-haloimidazolium halide substituent and counteranion respectively.<sup>55,94,55</sup> <sup>b</sup> Z' = 2. <sup>c</sup> X...A<sup>−</sup> distance refers to the shortest the distance between the iodoimidazolium iodine atom and the closest of the four phosphate oxygen atoms.

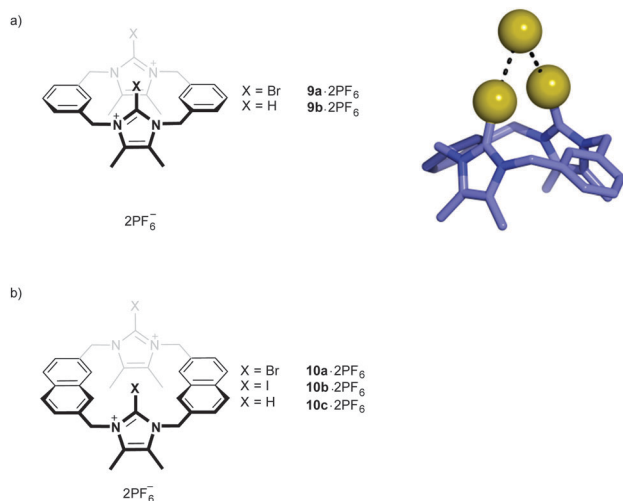


**Fig. 8** Beer's haloimidazoliophane receptors: (a) chemical structure of the xylyl-containing bromoimidazolium-functionalised macrocycle **9a-2PF<sub>6</sub>** and solid state structure of the bromide complex **9a-2Br**; hydrogen atoms, solvent molecules and the non-coordinating bromide counteranion have been omitted for clarity; halogen-bonding interactions shown as dashed lines; (b) chemical structures of extended naphthyl-containing bromo-, iodo- and proto-imidazolium analogues.

All three of the macrocyclic receptors **9a-2PF<sub>6</sub>**, **10a-2PF<sub>6</sub>** and **10b-2PF<sub>6</sub>** show markedly enhanced halide binding affinities compared to their protoimidazolium-functionalised HB analogues **9b-2PF<sub>6</sub>** and **10c-2PF<sub>6</sub>** (Fig. 8). The *syn* atropisomer of the *meta*-xylyl bromoimidazoliophane macrocycle **9a-2PF<sub>6</sub>** was found to display an unusually pronounced selectivity for Br<sup>−</sup> ( $K_a = 889 \text{ M}^{-1}$ ) among the halide anions<sup>56</sup> (Table 2), which was attributed to an interplay between steric and geometric factors.<sup>60</sup> Replacement of the xylyl spacer with an extended naphthalene spacer in **10a-2PF<sub>6</sub>** resulted in significantly higher affinities for the heavier halides, with a reversal in the Br<sup>−</sup> over I<sup>−</sup> selectivity exhibited by receptor **9a-2PF<sub>6</sub>**. Conversely the, naphthyl-containing bis-iodoimidazoliophane macrocycle **10b-2PF<sub>6</sub>** was found to complex Br<sup>−</sup> selectively over I<sup>−</sup>. Both of the naphthyl containing haloimidazoliophane receptors

§ According to common convention, we have used atomic van der Waals radii for anionic species because these parameters are relatively well-defined and self-consistent compared to anionic radii. Where the relevant data exist, values for anionic and van der Waals radii appear to be similar.<sup>99</sup>

**Table 2** Association constants,  $K_a$  (M<sup>−1</sup>), for 1:1 complexes of receptors **9a**, **9b** and **10a–c** with halide anions in 9:1 CD<sub>3</sub>OD : D<sub>2</sub>O or CH<sub>3</sub>OH : H<sub>2</sub>O

	Cl <sup>−</sup>	Br <sup>−</sup>	I <sup>−</sup>
<b>9a-2PF<sub>6</sub></b> <sup>a</sup>	< 10	889	184
<b>9b-2PF<sub>6</sub></b> <sup>a</sup>	133	130	102
<b>10a-2PF<sub>6</sub></b> <sup>b</sup>	—	28 800	955 000
<b>10b-2PF<sub>6</sub></b> <sup>b</sup>	—	631 000	37 100
<b>10c-2PF<sub>6</sub></b> <sup>a</sup>	19	85	80

<sup>a</sup>  $K_a$  values obtained from <sup>1</sup>H NMR titration experiments in 9:1 CD<sub>3</sub>OD : D<sub>2</sub>O at 293–5 K. <sup>b</sup>  $K_a$  values obtained from fluorescence titration experiments at 293 K. Anions added as TBA salts. Estimated errors < 10%.

showed negligible affinities for a range of smaller halide and oxoanions and were able to exclusively sense Br<sup>−</sup> and I<sup>−</sup> *via* enhancements in their fluorescence emission spectra. X-ray crystallographic studies in combination with computational density functional theory and molecular dynamics simulations supported the formation of stable receptor-halide complexes in solution mediated by cooperative bidentate XB donation from the receptors' haloimidazolium groups to the guest anion. Although dimeric 2:2 receptor:anion complexes were observed in the solid state structures of **10b-Br-PF<sub>6</sub>** and **10b-I-PF<sub>6</sub>**, <sup>1</sup>H NMR Job-plot and DOSY NMR experiments indicated that monomeric 1:1 receptor:halide complexes are preferred in solution.<sup>57</sup>

The groups of Ghosh<sup>61</sup> and Berryman<sup>62</sup> have incorporated iodoimidazolium XB-donor motifs into preorganised bipodal and tripodal host molecules (Fig. 9) which were shown to be capable of recognising halide anions in CD<sub>3</sub>CN/D<sub>2</sub>O mixtures and CH<sub>3</sub>CN respectively. The differing halide selectivity trends displayed by the bipodal (Cl<sup>−</sup> > Br<sup>−</sup> > I<sup>−</sup>) and tripodal (Br<sup>−</sup> > Cl<sup>−</sup> > I<sup>−</sup>) systems are presumably dictated by geometric and size-complementary factors. X-ray structural characterisation of the halide or mixed halide/hexafluorophosphate salts of each of these receptors confirmed the presence of strong C-I...X<sup>−</sup> XB interactions in the solid state. Furthermore it was demonstrated that the bromide salt of the tripodal receptor **12-2PF<sub>6</sub>** can be selectively crystallised from a DCM/DMF solution in the presence of a range of competing guest anions.

The potent XB-donor ability of the 2-iodoimidazolium motif has been exploited by Huber for organocatalysis applications.<sup>63</sup> The preorganised bis(iodobenzimidazolium) compound **13-2OTf** showed very strong catalytic activity in the benchmark halide-abstraction-type reaction of 1-chloroisochroman with a silyl enol

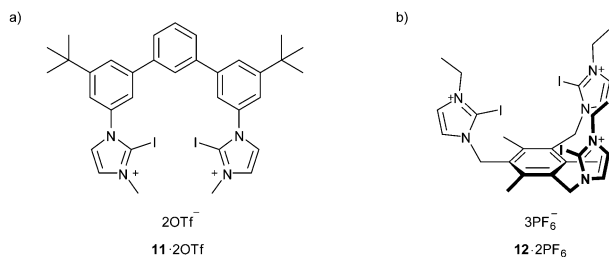
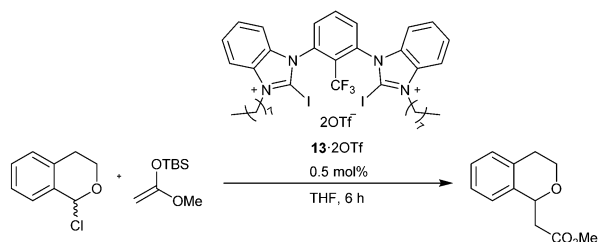


Fig. 9 Multidentate iodoimidazolium XB anion receptor's: (a) Ghosh's bipodal iodoimidazolium system and (b) Berryman's tripodal system.



Scheme 1 Catalysis of a benchmark halide extraction reaction using a bidentate iodoimidazolium XB anion receptor molecule.

ether (Scheme 1), affording the product in 70% yield with a catalyst loading of just 0.5 mol%. Calorimetric titration experiments, along with DFT calculations, demonstrated that compound **13-2OTf** is able to recognise  $\text{Cl}^-$  anions with high affinity ( $K_a = 3.5 \times 10^6 \text{ M}^{-1}$  in  $\text{CH}_3\text{CN}$ ) *via* the formation of cooperative bidentate  $\text{C-I} \cdots \text{Cl}^-$  halogen bonds, which was proposed as a rationale for its exceptionally high organocatalytic activity.

### Halotriazole and halotriazolium receptors

Halotriazole and halotriazolium motifs have recently attracted much attention as XB analogues of the widely studied and readily synthetically accessible C–H hydrogen-bond-donating

triazole<sup>64</sup> and triazolium<sup>65,66</sup> anion recognition motifs. A number of computational and experimental studies have indicated that the XB donor ability of these halotriazole-based systems increases with increasing size of the halogen substituent ( $\text{I} > \text{Br} > \text{Cl}$ );<sup>67,68</sup> it has also been shown by theory and experiment that the cationic halotriazolium motif is a more effective XB donor than the charge neutral halotriazole motif,<sup>67–69</sup> which can be attributed to the combined effects of charge assistance and greater C–X bond polarisation. The incorporation of multiple chelating iodotriazole motifs onto preorganised scaffolds has nonetheless proven to be an effective approach to anion receptor design. Schubert *et al.* prepared a bidentate receptor (**14**) in which a carbazole scaffold is symmetrically functionalised with hydroxyl and iodotriazole units in the 2 and 3 positions respectively (Fig. 10a). An X-ray crystal structure, along with solution NMR experiments, indicated that intramolecular  $\text{O-H} \cdots \text{N}$  HB interactions between the hydroxyl and iodotriazole groups preorganise the triazole into a co-planar *syn-syn* conformation which favours cooperative bidentate anion recognition, minimising the need for conformational reorganisation of the host prior to anion complexation. The  $\text{Cl}^-$  and  $\text{Br}^-$  binding properties of this receptor were probed *via* isothermal titration calorimetry experiments in THF: both anions are complexed in a 2 : 1 receptor : anion binding mode with similar magnitudes of association constant, and with favourable enthalpic and entropic contributions to the overall free energy of binding. The favourable effect of preorganisation is evident from a comparison to receptor **15** which exhibits significantly lower  $\text{Cl}^-$  and  $\text{Br}^-$  binding affinities, primarily as a result of the greater entropic penalty associated with the formation of the receptor-halide complex.<sup>70</sup> In the bimetallic bis-iodotriazole pyrimidine derivative **16a** the chelation of the two  $\text{Re}(\text{I})$  centres serves to preorganise the iodotriazole groups as well as conceivably increasing the degree of polarisation of the C–I bonds (Fig. 10b). This receptor's binding affinities and selectivities for a range of halide and oxoanions differ significantly from those

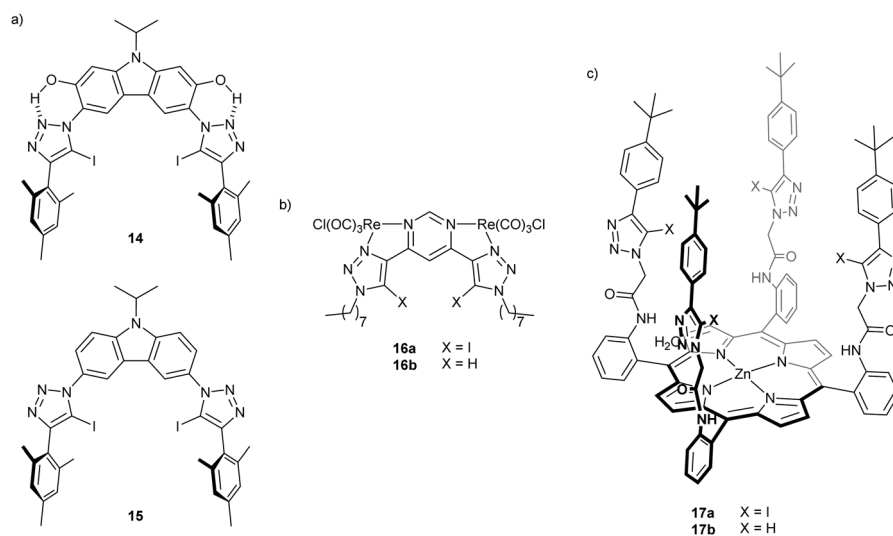
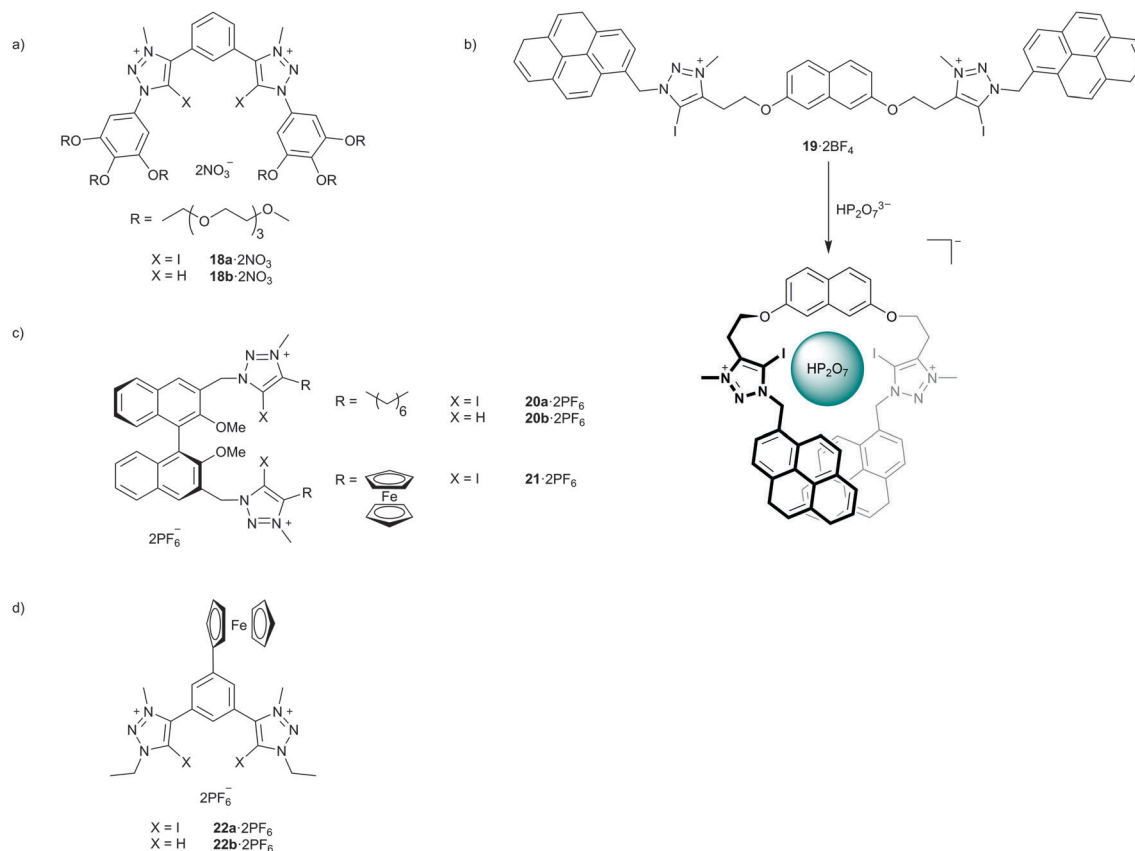


Fig. 10 Examples of preorganised multidentate XB anion receptors based on the iodotriazole motif: (a) Schubert's carbazole-bridged bipodal receptor; (b) Beer's bi-metallic pyrimidine-bridged bis-iodotriazole receptor and (c) a tetrapodal receptor in which four iodotriazole groups are pendant from a  $\text{Zn}(\text{II})$  porphyrin scaffold.

of the hydrogen bonding bis-prototriazole analogue **16b**. While the halide, hydrogen carbonate and acetate binding affinities of the XB receptor **16a** in  $\text{CDCl}_3:\text{CD}_3\text{OD}$  1:1 are significantly enhanced compared to those of the HB receptor **16b**, the HB receptor is a marginally superior complexant of  $\text{H}_2\text{PO}_4^-$ ,  $\text{ClO}_4^-$ ,  $\text{SO}_4^-$ , and  $\text{NO}_3^-$  anions. The HB receptor shows little discrimination among the monovalent anions ( $92 \leq K_a \leq 548 \text{ M}^{-1}$ ) while in contrast a marked selectivity for  $\text{I}^-$  ( $K_a > 10^4 \text{ M}^{-1}$ ) is observed in this series for the XB receptor.<sup>71</sup> The integration of four iodotriazole motifs onto a preorganised picket-fence-style  $\text{Zn}(\text{II})$  metalloporphyrin scaffold (Fig. 10c) allowed anion recognition to occur *via* multi-dentate  $\text{C-I} \cdots \text{X}$  XB interactions and simultaneous ligation of the anionic guest to the Lewis acidic  $\text{Zn}(\text{II})$  centre.<sup>72</sup> The anion recognition properties of the XB receptor **17a** and analogous HB receptor **17b** were investigated by UV-visible titration experiments in  $\text{CHCl}_3$ , acetone and acetonitrile. For both receptors a general preference for oxoanions over halide anions was observed, with the trend in halide binding affinities correlating with the charge density of the anion ( $\text{Cl}^- > \text{Br}^- > \text{I}^-$ ). Notably the XB receptor's halide binding affinities are invariably higher than those of the HB receptor across all three solvents, while the same trend is not observed for oxoanions. Intriguingly the anion binding capabilities of both the XB and HB receptor showed an emphatic dependence on the choice of solvent (acetone > acetonitrile > chloroform).

Utilisation of the more potent cationic iodotriazolium XB motif has enabled the construction of anion host molecules which are capable of recognising and sensing environmentally and biologically relevant anions. The development of receptors which recognise a target anionic substrate with high degree of selectivity in aqueous media is of paramount importance for medical and environmental applications but the high solvation energies of anions in water present a major impediment to this goal.<sup>73,74</sup> The bis-iodotriazolium receptor **18a**· $2\text{NO}_3$  (Fig. 11a), rendered water soluble by the attachment of six peripheral tetraethylene glycol substituents, was used to probe XB-driven anion recognition processes in aqueous solution. This receptor's halide binding affinities, along with those of the HB analogue **18b**· $2\text{NO}_3$ , show the expected Hofmeister bias ( $\text{I}^- > \text{Br}^- > \text{Cl}^-$ ) in  $\text{D}_2\text{O}$ , correlating with the relative ease of desolvation of the heavier halides. Interestingly however the XB receptor is able to recognise  $\text{ReO}_4^-$  ( $K_a = 44 \text{ M}^{-1}$ ;  $\Delta G_{\text{hyd}} = -330 \text{ kJ mol}^{-1}$ ), a model for the radioactive pertechnetate anion, with comparable affinity to  $\text{I}^-$  ( $K_a = 51 \text{ M}^{-1}$ ;  $\Delta G_{\text{hyd}} = -275 \text{ kJ mol}^{-1}$ ). In striking contrast the HB receptor **18b**· $2\text{NO}_3$  displays no appreciable binding affinity for  $\text{ReO}_4^-$ . van't Hoff analysis demonstrated that the complexation of  $\text{ReO}_4^-$  to **18a**· $2\text{NO}_3$  is enthalpically driven ( $\Delta H = -12 \text{ kJ mol}^{-1}$ ) and entropically disfavoured ( $T\Delta S = -2.7 \text{ kJ mol}^{-1}$ ), which is characteristic of a chaotropic<sup>75</sup> or non-classical hydrophobic effect<sup>76,77</sup> and may also provide an indication



**Fig. 11** Iodotriazolium-based XB anion complexants: (a) Beer's water-soluble perrhenate receptor; (b) Molina and co-workers' pyrene-functionalised bis-iodotriazolium receptor; (c) Beer's enantioselective receptor based on an (S)-BINOL scaffold and (d) Beer's electrochemical halide sensor.

that the exothermic formation of C–I...O XB interactions plays a pivotal role in driving the association process. In addition the complexation of  $\text{ReO}_4^-$  by the XB receptor **18a**·2NO<sub>3</sub> in aqueous HEPES buffer is signalled by an enhancement in fluorescence emission intensity.<sup>78</sup> Similarly, the pyrene-functionalised bis-iodotriazolium compound **19**·2BF<sub>4</sub> (Fig. 11b) is a selective fluorescent chemosensor for biologically relevant pyrophosphate anions, which induce an enhancement in the emission intensity of the pyrene excimer band in acetone. With the aid of computational modelling, this observation was ascribed to a XB-mediated conformational rearrangement upon hydrogen pyrophosphate complexation.<sup>79</sup> In the first example of the application of XB interactions to enantioselective anion recognition, we appended two convergent iodotriazolium motifs onto a chiral, enantiopure (S)-BINOL core. The resulting dicationic XB receptor **20a**·2PF<sub>6</sub> (Fig. 11c) is able to recognise a range of chiral amino acid carboxylate or BINOL-phosphate anions with higher affinities and enhanced enantioselectivities compared to the bis-prototriazolium HB analogue **20b**·2PF<sub>6</sub> in CD<sub>3</sub>CN:D<sub>2</sub>O 99:1.<sup>80</sup> Indeed the HB receptor exhibited almost no enantiodiscrimination capabilities for all of the chiral anion pairs which were investigated. For the XB receptor, the greatest enantioselectivity was observed for the *N*Boc-tryptophan anion ( $K_S/K_R = 1.67$ ), which bears a sterically bulky indole substituent. Computational MD simulations and DFT calculations indicated that steric factors, in combination with the strict linearity of the receptor...anion XB interactions, provide a rationale for the experimentally observed enantioselective anion binding properties of receptor **20a**·2PF<sub>6</sub>. An analogous ferrocene-functionalised XB receptor (**21**·2PF<sub>6</sub>) was shown by means of square-wave voltammetry experiments in CH<sub>3</sub>CN to selectively sense the more strongly bound enantiomers of *N*Boc-alanine, *N*Boc-leucine and BINOL-PO<sub>4</sub> *via* larger cathodic shifts in the receptor's ferrocene/ferrocenium redox couple. Likewise, cyclic voltammetry experiments revealed that the related ferrocene-appended bis-iodotriazolium receptor **22a**·2PF<sub>6</sub> (Fig. 11d) is capable of electrochemically sensing Cl<sup>−</sup> and Br<sup>−</sup> anions in CH<sub>3</sub>CN and CH<sub>3</sub>CN/H<sub>2</sub>O mixtures *via* halide-anion-induced cathodic perturbations ( $\Delta E_{1/2} = 12\text{--}32$  mV) of the ferrocene/ferrocenium redox couple. Under the same experimental conditions the cathodic perturbations which were measured for the HB receptor **22b**·2PF<sub>6</sub> were appreciably smaller in magnitude ( $\Delta E_{1/2} = 6\text{--}17$  mV). A tentative explanation for the enhanced electrochemical sensing abilities of the XB receptor compared to the HB analogue is that a significant covalent contribution to the receptor...anion XB interactions gives rise to a more effective through-bond-communication pathway between the ferrocene reporter group and the bound halide anion.<sup>81</sup>

### Mechanically interlocked halogen bonding anion receptors

Within our group we have developed a research programme designed to exploit the unique binding pockets contained within mechanically interlocked rotaxane and catenane molecules for anion recognition and sensing purposes.<sup>82,83</sup> The use of interlocked host molecules is an attractive means of overcoming the specific challenges associated with the complexation of anionic guests for multiple reasons: this approach facilitates the design and

construction of complex, three-dimensional binding cavities which possess optimal size- and shape-complementarity for a target guest species; the shielded, hydrophobic nature of these interlocked binding domains assists in the desolvation of the bound guest species—an essential prerequisite for effective anion recognition in aqueous media given the high hydration energies of anions in water; secondary stabilising interactions between the interlocked components can be used to confer favourable preorganisation upon the host system, while importantly maintaining a degree of flexibility; the dynamic properties of these systems can be exploited in order to achieve a sensory readout response upon guest binding when appropriate reporter groups are incorporated. As an extension of our previous work on HB interlocked host systems, we have recently incorporated XB donor groups into a range of [2]rotaxane and [2]catenane architectures, the majority of which have shown contrasting and often superior anion recognition properties compared to HB analogues.

### Development of interlocked host systems containing convergent hydrogen- and halogen-bond-donor groups

In 2010 we reported the first XB interlocked host system: a [2]rotaxane in which a bidentate isophthalamide HB donor motif and iodotriazolium XB donor group from the macrocycle and axle components respectively converge towards a central binding cavity (**23a**·PF<sub>6</sub>, Fig. 12). An X-ray crystal structure of

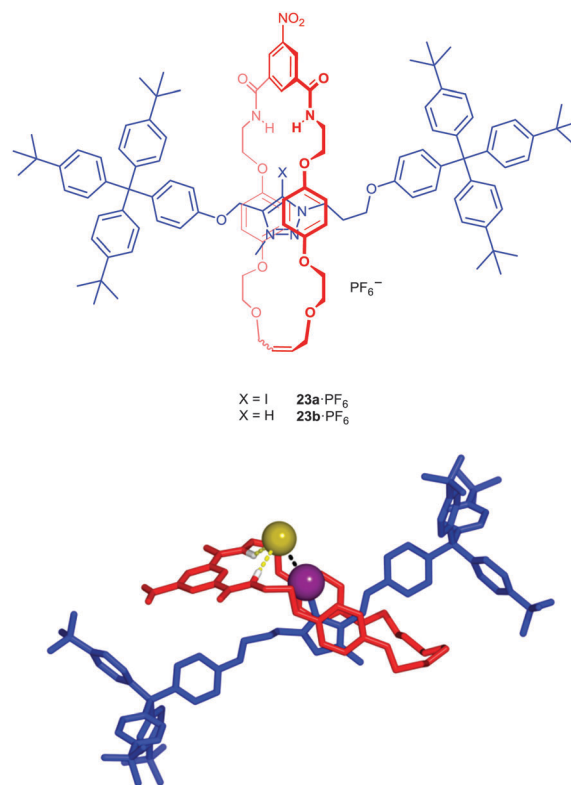


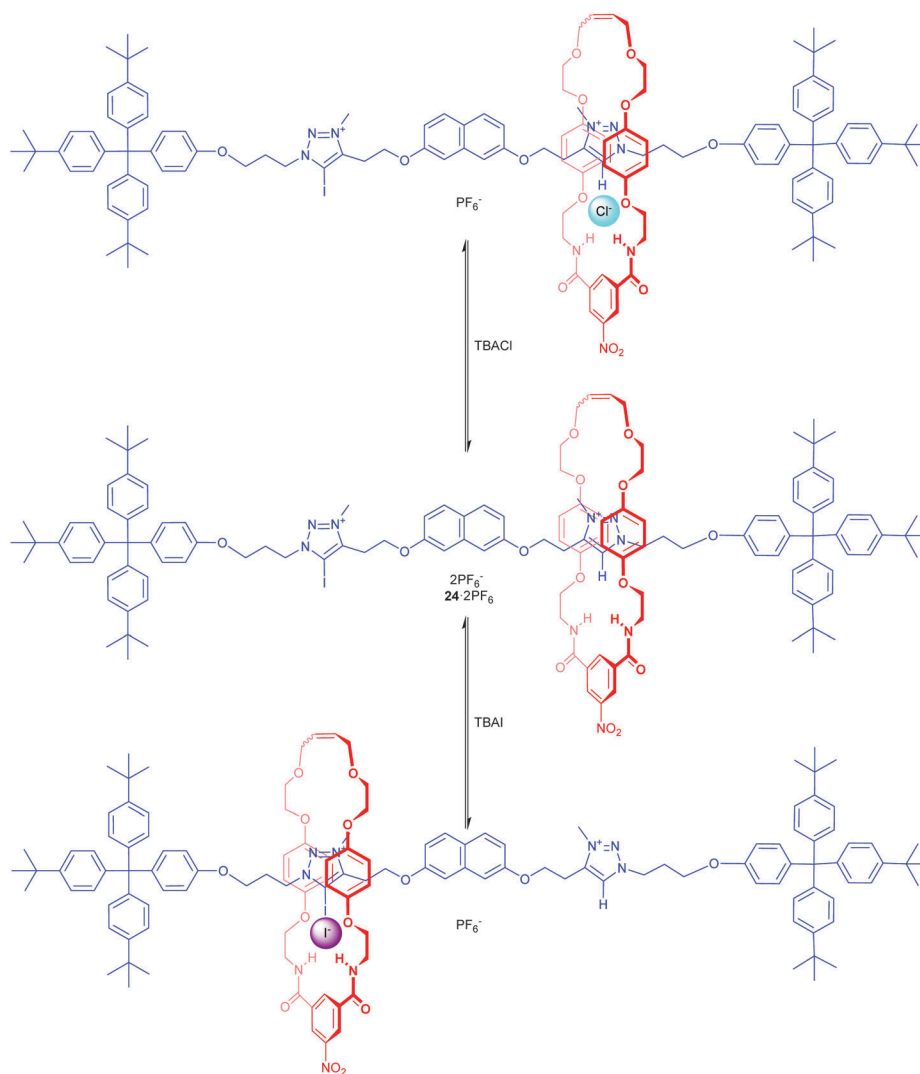
Fig. 12 Chemical structure (above) and solid state structure (bottom) of Beer's [2]rotaxane containing an iodotriazolium-functionalised axle component. For clarity non-polar hydrogen atoms have been omitted from the representation of the solid state structure. The halogen bond and hydrogen bonds are represented as black and yellow dashed lines respectively.



the rotaxane-bromide complex confirmed that the halide guest is encapsulated within the rotaxane's interlocked binding cavity by three complementary hydrogen- and halogen-bonding interactions (Fig. 12). Solution phase anion binding investigations revealed that the halide binding affinities of this system are significantly enhanced compared to those of the HB analogue **23b**-PF<sub>6</sub>.<sup>84</sup> Furthermore the XB rotaxane showed an overall preference for I<sup>−</sup> ( $K_a(\text{I}^-) = 2228 (171) \text{ M}^{-1}$ ;  $K_a(\text{Br}^-) = 1251 (10) \text{ M}^{-1}$ ;  $K_a(\text{Cl}^-) = 457 (4) \text{ M}^{-1}$ ) in CDCl<sub>3</sub>:CD<sub>3</sub>OD:D<sub>2</sub>O 45:45:10 while a reversal in this trend is observed for the HB rotaxane in a similar CDCl<sub>3</sub>:CD<sub>3</sub>OD 1:1 solvent mixture. A follow-up study on a series of related bromotriazolium and iodotriazolium [2]rotaxane host systems revealed that the halide binding affinities of these systems increase with increasing intercomponent preorganisation, and with increasing polarisability and XB donor atom (I > Br).<sup>85</sup> Meanwhile the orthogonal halide selectivity behaviour displayed by the XB and HB rotaxanes **23a**-PF<sub>6</sub> and **23b**-PF<sub>6</sub> was exploited for the control of molecular motion in the two-station rotaxane molecular

shuttle **24**-2PF<sub>6</sub>, which incorporates both iodotriazolium and prototriazolium motifs in the axle constituent. The macrocycle component was found to preferentially reside at the axle prototriazolium station in the absence of coordinating anions and in the presence of Cl<sup>−</sup> but the addition of I<sup>−</sup> induced a change in co-conformation, with the macrocycle shuttling to the iodotriazolium station, driven by the formation of cooperative C-I...I<sup>−</sup> XB and N-H...I<sup>−</sup> HB interactions (Scheme 2).

A rotaxane incorporating a pyridinium iodotriazole XB donor group (**25a**-PF<sub>6</sub>, Fig. 13a) was discovered to bind halides preferentially over H<sub>2</sub>PO<sub>4</sub><sup>−</sup> and AcO<sup>−</sup> anions in 1:1 CDCl<sub>3</sub>:CD<sub>3</sub>OD in contrast to the HB prototriazole-containing analogue **25b**-PF<sub>6</sub>, which is selective for H<sub>2</sub>PO<sub>4</sub><sup>−</sup>.<sup>86</sup> The calculated anion association constants for the HB rotaxane are consistently higher than those for the XB system, suggesting that anion complexation to the XB rotaxane may be sterically inhibited by the presence of the bulky iodine substituent. Mixed hydrogen- and halogen-bonding catenanes incorporating an alternative



**Scheme 2** Iodide induced molecular motion in a mixed hydrogen- and halogen-bonding two-station rotaxane shuttle. (Solvent: CDCl<sub>3</sub>:CD<sub>3</sub>OD 1:1. Temperature: 295 K).

halopyridinium XB donor group were also investigated.<sup>87</sup> Both the bromopyridinium- and iodopyridinium-functionalised [2]catenanes **26a**·PF<sub>6</sub> and **26b**·PF<sub>6</sub> were observed to bind halides (I<sup>−</sup> > Br<sup>−</sup> > Cl<sup>−</sup>) selectively over AcO<sup>−</sup> in CDCl<sub>3</sub>:CD<sub>3</sub>OD 1:1, with the iodopyridinium system **26b**·PF<sub>6</sub> proving to be a marginally superior halide complexant than the bromopyridinium analogue **26a**·PF<sub>6</sub> (Fig. 13b).

### Incorporation of multiple chelating halogen bond donor groups

Expanding upon this early work, we turned to the incorporation of multiple convergent XB donor groups into interlocked structural frameworks in an effort to further enhance anion binding affinities and modulate selectivities. A rotaxane incorporating a HB isophthalamide-functionalised macrocycle component along with an axle constituent in which two XB iodotriazolium groups are separated by a rigid carbazole spacer (**27**·2PF<sub>6</sub>, Fig. 14a) showed a remarkably high selectivity for the halides over AcO<sup>−</sup> and H<sub>2</sub>PO<sub>4</sub><sup>−</sup> anions in CDCl<sub>3</sub>:CD<sub>3</sub>OD:D<sub>2</sub>O 45:45:10, with Br<sup>−</sup> being bound with particularly high affinity ( $K_a > 10^4 \text{ M}^{-1}$ ).<sup>88</sup>

The bidentate 3,5-bis-(iodotriazole)-pyridinium motif was incorporated into a mixed hydrogen- and halogen-bonding [2]catenane host structure (**28a**·PF<sub>6</sub>, Fig. 14b(i)) using a chloride-anion templated ring-closing metathesis ‘clipping’ reaction. This receptor showed markedly enhanced halide binding affinities compared to the all hydrogen-bonding catenane **28b**·PF<sub>6</sub>, and a strong preference for I<sup>−</sup> and Br<sup>−</sup> over the smaller Cl<sup>−</sup> anion in a competitive aqueous-organic CDCl<sub>3</sub>/CD<sub>3</sub>OD/D<sub>2</sub>O solvent mixture (Table 3).

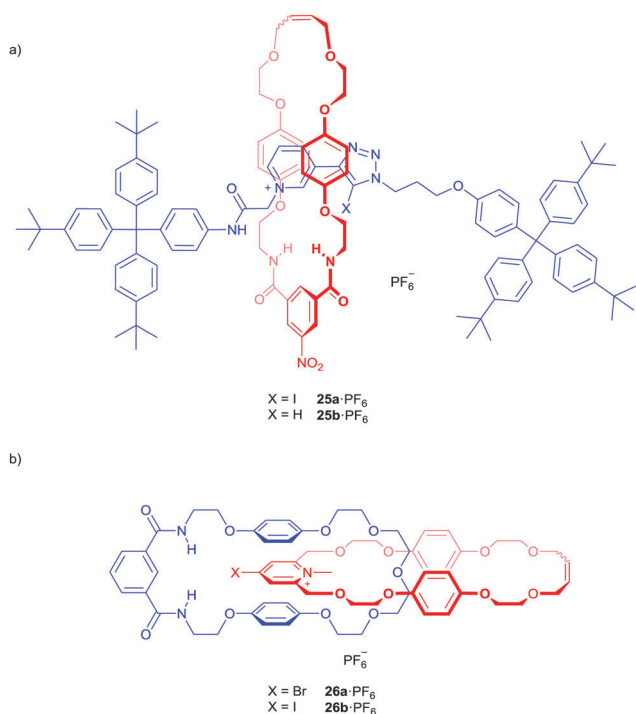


**Fig. 13** (a) Further examples of mixed XB/HB interlocked host systems: (a) a [2]rotaxane incorporating an isophthalamide macrocycle and a pyridinium iodotriazole-based axle component; (b) [2]catenanes incorporating convergent isophthalamide and halopyridinium anion recognition motifs.

Interestingly the XB [2]catenane **28a**·PF<sub>6</sub> showed no measurable solution binding affinities for the oxoanions AcO<sup>−</sup> and H<sub>2</sub>PO<sub>4</sub><sup>−</sup>, while in contrast a less constrained acyclic bis-(iodotriazole)-pyridinium model system (**29**·PF<sub>6</sub>, Fig. 14b(ii)) binds AcO<sup>−</sup> in preference to halide anions, albeit in a dissimilar aprotic DMSO-d<sub>6</sub> solvent environment. The formation of a complementary

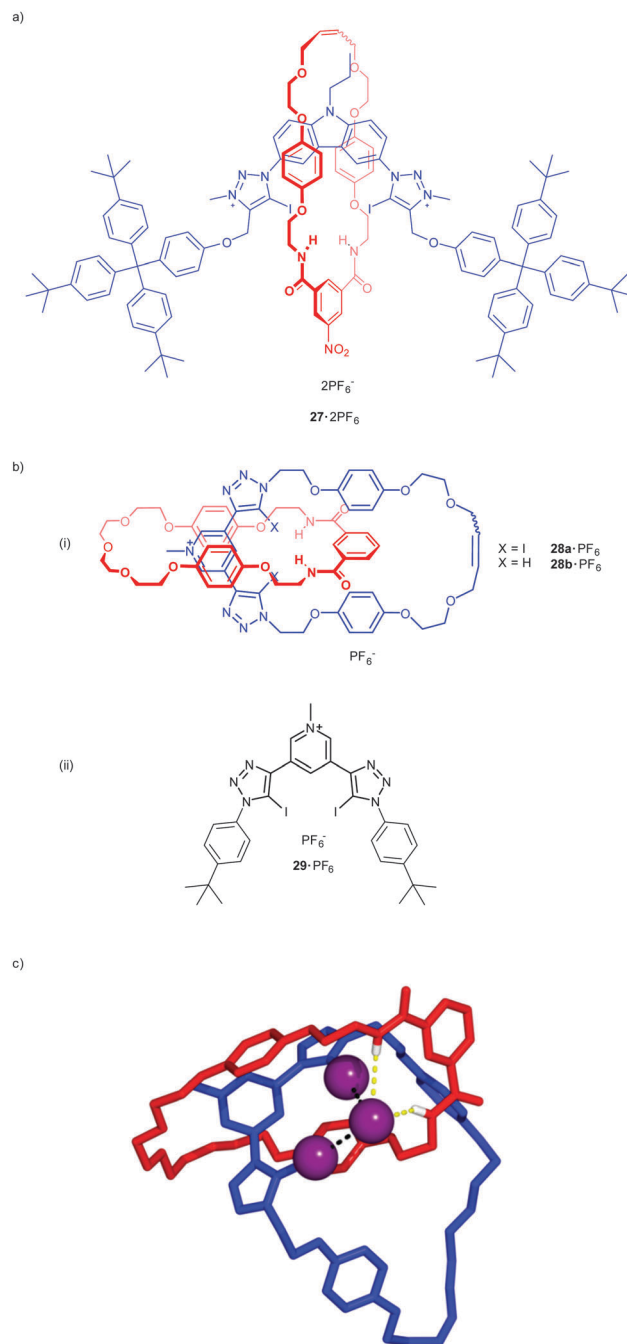


**Fig. 14** Interlocked host structures incorporating multiple chelating XB donor groups: (a) a [2]rotaxane incorporating two axle iodotriazolium groups bridged by a rigid carbazole spacer; (b) (i) a [2]catenane incorporating a bidentate bis-(iodotriazole)pyridinium XB donor motif and (ii) an acyclic model system; (c) solid state structure of the iodide complex of the [2]catenane **28a**·PF<sub>6</sub>. Non-polar hydrogen atoms have been omitted for clarity. Halogen and hydrogen bonds represented as black and yellow dashed lines respectively.

array of receptor–anion XB and HB interactions is manifest in the isomorphous solid state structures of the three catenane-halide complexes (Fig. 14c). Importantly, intense pre-edge features were observed in the Cl and Br K edge X-ray absorption spectra of the [2]catenane complexes **28a**-Cl and **28a**-Br, indicating a significant degree of covalent charge-transfer from the bound halide counter-anion to the XB donor atom.<sup>89</sup>

Functionalisation of the bis-iodotriazole pyridinium motif with permethylated  $\beta$ -cyclodextrin stoppering groups allowed us to synthesise a fully water soluble dicationic [2]rotaxane analogue of this catenane host system (Fig. 15a) using an established anion-templated, amide-condensation based clipping methodology.<sup>90,91</sup> <sup>1</sup>H NMR anion binding titration experiments revealed that, while the halide and sulfate anion recognition capabilities of the all-hydrogen-bonding bis-prototriazole-functionalised [2]rotaxane **30b**-2NO<sub>3</sub> in pure D<sub>2</sub>O are modest,

the hybrid hydrogen- and halogen-bonding [2]rotaxane **30a**-2NO<sub>3</sub> exhibits notably superior anion recognition properties. In particular, the I<sup>−</sup> binding affinity of the XB rotaxane **30a**-2NO<sub>3</sub> ( $\Delta G = -19$  kJ mol<sup>−1</sup>) is dramatically amplified compared that of rotaxane **30b**-2NO<sub>3</sub> ( $\Delta G = -7$  kJ mol<sup>−1</sup>) (Table 4). van't Hoff analysis revealed fundamental differences between the thermodynamic contributions to the XB- and HB-driven I<sup>−</sup> recognition process for rotaxanes **30a**-2NO<sub>3</sub> and **30b**-2NO<sub>3</sub> respectively: in the case of the HB rotaxane **30b**-2NO<sub>3</sub> iodide complexation is entropically driven and enthalpically disfavoured suggesting that a classical hydrophobic effect may be in operation, with the positive entropic term reflecting the release of D<sub>2</sub>O molecules from the host and guest upon anion binding; conversely the recognition of I<sup>−</sup> by the bis-iodotriazole-functionalised rotaxane **30a**-2NO<sub>3</sub> is entropically unfavourable and driven by a favourable enthalpic term, which may signify the critical importance of the formation of strongly exothermic C–I ⋯ I<sup>−</sup> XB interactions. It was subsequently shown that a related tricationic [2]rotaxane host system incorporating an integral Ru(II) bipyridyl luminescent reporter group (**31**-3NO<sub>3</sub>, Fig. 15b) is able to recognise I<sup>−</sup> with higher affinity ( $K_a = 6300$  M<sup>−1</sup>) in D<sub>2</sub>O, with the recognition process being signalled by a 6% enhancement in the intensity of the Ru-centred MLCT emission band.<sup>92</sup>

### All halogen-bonding interlocked host systems

As a natural development of this work we have also investigated interlocked host systems which are capable of recognising guest anions solely *via* cooperative XB interactions. Using a bromide anion templated double clipping reaction we prepared the symmetrical 2-bromoimidazolium homo[2]catenane **32**-2PF<sub>6</sub>,

**Table 3** Association constants,  $K_a$  (M<sup>−1</sup>), for 1:1 complexes of receptors **28a**-PF<sub>6</sub>, **28b**-PF<sub>6</sub> and **29**-PF<sub>6</sub> with various halide and oxoanions

	<b>28a</b> -PF <sub>6</sub> <sup>a</sup>	<b>28b</b> -PF <sub>6</sub> <sup>b</sup>	<b>29</b> -PF <sub>6</sub> <sup>c</sup>
Cl <sup>−</sup>	1850 (224)	680(20)	387 (20)
Br <sup>−</sup>	> 10 <sup>4</sup>	630(50)	238 (120)
I <sup>−</sup>	> 10 <sup>4</sup>	510(10)	146 (3)
AcO <sup>−</sup>	NB <sup>d</sup>	—	1025 (9)
H <sub>2</sub> PO <sub>4</sub> <sup>−</sup>	NB <sup>d</sup>	49(4)	NB <sup>d</sup>

Association constant values determined using <sup>1</sup>H NMR titration experiments. All anions added as TBA salts. Estimated standard errors are given in parentheses. <sup>a</sup> In CDCl<sub>3</sub>:CD<sub>3</sub>OD:D<sub>2</sub>O 45:45:10 at 293 K. <sup>b</sup> In CDCl<sub>3</sub>:CD<sub>3</sub>OD 1:1 at 298 K. <sup>c</sup> In DMSO-d<sub>6</sub> at 298 K. <sup>d</sup> NB: No binding.

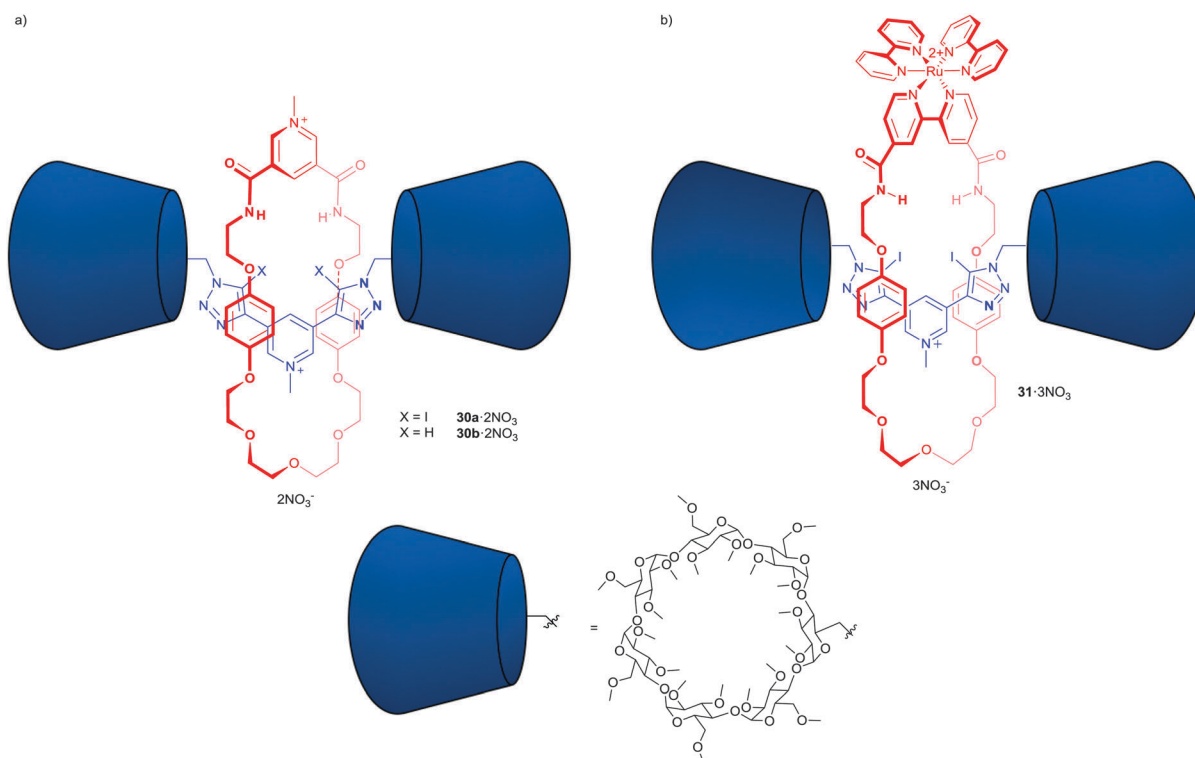


**Fig. 15** Water soluble hybrid XB/HB [2]rotaxane anion host systems: (a) a dicationic prototype and (b) a Ru(II) bipyridyl-functionalised tricationic variant.

**Table 4** Association constants,  $K_a$  ( $M^{-1}$ ), for 1:1 complexes of receptors **30a**·2NO<sub>3</sub> and **30b**·2NO<sub>3</sub> with halide and sulfate anions in D<sub>2</sub>O and thermodynamic parameters for I<sup>−</sup> binding

		$K_a^a$ ( $M^{-1}$ )	$\Delta G$ ( $kJ\ mol^{-1}$ )	$\Delta H^b$ ( $kJ\ mol^{-1}$ )	$T\Delta S^b$ ( $kJ\ mol^{-1}$ )
<b>30a</b> ·2NO <sub>3</sub>	Cl <sup>−</sup>	55	−10	—	—
	Br <sup>−</sup>	290	−14	—	—
	I <sup>−</sup>	2200	−19	−34	−15
	SO <sub>4</sub> <sup>2−</sup>	30	−8	—	—
<b>30b</b> ·2NO <sub>3</sub>	Cl <sup>−</sup>	NB <sup>c</sup>	—	—	—
	Br <sup>−</sup>	10	−6	—	—
	I <sup>−</sup>	20	−7	13	21
	SO <sub>4</sub> <sup>2−</sup>	NB <sup>c</sup>	—	—	—

<sup>a</sup> Association constants determined using <sup>1</sup>H NMR titration experiments at 298 K. Errors estimated to be <10%. <sup>b</sup>  $\Delta H$  and  $\Delta T$  values determined by van't Hoff analysis of data obtained from variable temperature <sup>1</sup>H NMR titration experiments. Errors estimated to be <15%. All anions added as sodium salts. <sup>c</sup> NB: No binding.

(Fig. 16a) which is able to recognise and sense Cl<sup>−</sup> and Br<sup>−</sup> anions exclusively among a series of other halide and oxoanions in CH<sub>3</sub>CN through the formation of two convergent charge assisted C–Br<sup>−</sup>···A<sup>−</sup> XB interactions.<sup>93</sup> Addition of Cl<sup>−</sup> and Br<sup>−</sup> anions to CH<sub>3</sub>CN solutions of the [2]catenane caused characteristic changes in the monomer and excimer emission bands associated with the fluorescent naphthalene reporter group. Association constants of  $K_a = 3.71 \times 10^6\ M^{-1}$  and  $K_a = 1.48 \times 10^5\ M^{-1}$  for Cl<sup>−</sup> and Br<sup>−</sup> respectively were determined using quantitative fluorescence titration experiments. In contrast, no spectral perturbations were observed upon addition of F<sup>−</sup>, I<sup>−</sup>, AcO<sup>−</sup>, H<sub>2</sub>PO<sub>4</sub><sup>−</sup>, NO<sub>3</sub><sup>−</sup> and HCO<sub>3</sub><sup>−</sup> anions, which presumably indicates that the precise arrangement of the XB donor groups in the [2]catenane's highly preorganised binding cavity does not complement the radii and geometries of these potential guest anions.

An all-halogen-bonding luminescent [2]rotaxane (**33**·2PF<sub>6</sub>, Fig. 16b) for which guest-anion-recognition is mediated by four convergent iodotriazole and iodotriazolium XB-donor groups was similarly shown to selectively sense Cl<sup>−</sup>, Br<sup>−</sup> and I<sup>−</sup> anions in preference to F<sup>−</sup>, AcO<sup>−</sup>, H<sub>2</sub>PO<sub>4</sub><sup>−</sup>, NO<sub>3</sub><sup>−</sup> and HCO<sub>3</sub><sup>−</sup>, NO<sub>3</sub><sup>−</sup>, ClO<sub>4</sub><sup>−</sup> and SO<sub>4</sub><sup>2−</sup> anions in CH<sub>3</sub>CN/H<sub>2</sub>O solvent mixtures. The addition of the halide anions induced changes in the MLCT emission band associated with macrocycle component's integral Re(i) bipyridyl group. Impressively these halide anions are bound with high affinities ( $2.71 \leq \log K \leq 4.38$ ; I<sup>−</sup> > Br<sup>−</sup> > Cl<sup>−</sup>) in a highly competitive 1:1 CH<sub>3</sub>CN:H<sub>2</sub>O solvent mixture. An X-ray crystal structure of the chloride salt **33**·2Cl confirmed the existence of strong XB interactions between the rotaxane's iodotriazole and iodotriazolium XB donor groups and the Cl<sup>−</sup> counteranions in the solid state, with C–I···Cl<sup>−</sup> XB distances 15–21% shorter than the sum of the atomic van der Waals radii of chloride and iodine.<sup>55,94</sup>

We recently described the use of a Cu(i)-mediated active metal templation strategy to prepare a neutral all-halogen-bonding

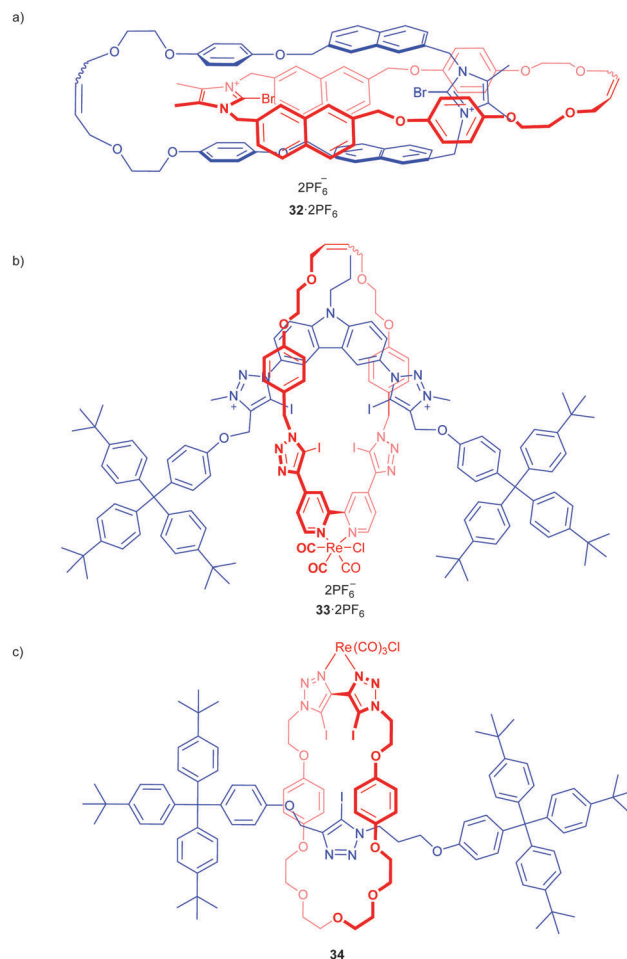


**Fig. 16** All halogen-bonding interlocked host systems: (a) a bromoimidazolium homo[2]catenane; (b) a dicationic [2]rotaxane incorporating an array of four preorganised iodotriazole/iodotriazolium XB donor groups; (c) a neutral Re(i)-appended [2]rotaxane incorporating three convergent iodotriazole XB donor groups.

[2]rotaxane host system (**34**, Fig. 16c) which is equipped with three convergent iodotriazole XB-donor groups.<sup>95</sup> This host system displays an amplified selectivity for halide anions over AcO<sup>−</sup> in CHCl<sub>3</sub> compared to an acyclic Re(i)-complexed bis-iodotriazole model system. Interestingly the halide selectivity trend (Cl<sup>−</sup> > Br<sup>−</sup> > I<sup>−</sup>) opposes that of the majority of the cationic interlocked XB host systems mentioned above, suggesting an optimal size complementarity between the rotaxane's interlocked binding cavity and the Cl<sup>−</sup> anion as well as potential differences in competitive solvation effects arising from the use of the aprotic solvent CHCl<sub>3</sub> in this study. In contrast there was no evidence of a binding interaction between the metal-free analogue of rotaxane **34** and the halide anions, which highlights the pivotal role of the Re(i) centre in the preorganising and polarising the axle bis-iodotriazole XB donor groups.

## Conclusions

Halogen bonding is still an emergent area of research: until a decade ago its application to solution phase anion recognition

† According to common convention, we have used atomic van der Waals radii for anionic species because these parameters are relatively well-defined and self-consistent compared to anionic radii. Where the relevant data exist, values for anionic and van der Waals radii appear to be similar.<sup>99</sup>



processes had been almost completely unexplored. However it is evident from the examples highlighted above that rapid advances have been made in this area during the intervening years, and XB has been unequivocally shown to be a genuinely useful complement to other, more established non-covalent interactions in anion receptor design. For example, XB-based anion host molecules have repeatedly been found to rival and even outperform HB analogues, especially in the recognition of halide anions. XB...anion interactions have been successfully applied to transmembrane anion transport, catalysis, enantioselective anion recognition, the recognition of biologically relevant anions, the template-directed synthesis of mechanically interlocked supramolecules, and the control of nanoscale molecular motion in a two-station rotaxane shuttle. In addition the numerous experimental and theoretical studies into XB anion recognition processes have provided fundamental insights into this understudied class of interaction in solution. We are especially excited by the promising ability of XB-based host systems to operate effectively in competitive aqueous solvent media and believe that this discovery could be an important step towards the design of functional anion receptor molecules with real-world applications in the selective detection, removal and transportation of negatively charged species. However, there is still much work to be done in order to understand the full scope of XB interactions in anion coordination chemistry and establish a more complete set of design principles. Detailed investigations are required in order to discern the thermodynamic subtleties of XB-mediated anion recognition processes. In addition, the number and variety of XB-donor motifs which have been studied remains limited, and the prospect of using analogous  $\sigma$ -hole interactions involving elements from other p-block groups<sup>96</sup> is hitherto unrealised. Given the promising results obtained to date, we anticipate a rapid growth and evolution in the area of halogen bonding anion recognition over the coming years.

## Acknowledgements

We thank the ERC for funding under the European Union's Framework Programme (FP7/2007–2013) ERC Advanced Grant Agreement no. 267426.

## Notes and references

- N. H. Evans and P. D. Beer, *Angew. Chem., Int. Ed.*, 2014, **53**, 11716–11754.
- J. L. Sessler, P. Gale, W.-S. Cho, J. F. Stoddart, S. J. Rowan, T. Aida and A. E. Rowan, *Anion Receptor Chemistry*, The Royal Society of Chemistry, 2006.
- J. W. Pflugrath and F. A. Quiocho, *Nature*, 1985, **314**, 257–260.
- H. Luecke and F. A. Quiocho, *Nature*, 1990, **347**, 402–406.
- N. M. Koropatkin, H. B. Pakrasi and T. J. Smith, *Proc. Natl. Acad. Sci. U. S. A.*, 2006, **103**, 9820–9825.
- N. M. Koropatkin, D. W. Koppenaal, H. B. Pakrasi and T. J. Smith, *J. Biol. Chem.*, 2007, **282**, 2606–2614.
- G. Cavallo, P. Metrangolo, R. Milani, T. Pilati, A. Priimagi, G. Resnati and G. Terraneo, *Chem. Rev.*, 2016, **116**, 2478–2601.
- H. A. Bent, *Chem. Rev.*, 1968, **68**, 587–648.
- P. Murray-Rust and W. D. S. Motherwell, *J. Am. Chem. Soc.*, 1979, **101**, 4374–4376.
- N. Ramasubbu, R. Parthasarathy and P. Murray-Rust, *J. Am. Chem. Soc.*, 1986, **108**, 4308–4314.
- M. H. Kolář and P. Hobza, *Chem. Rev.*, 2016, **116**, 5155–5187.
- P. Metrangolo, G. Resnati, T. Pilati and S. Biella, in *Halogen Bonding*, ed. P. Metrangolo and G. Resnati, Springer Berlin Heidelberg, Berlin, Heidelberg, 2008, vol. 126, pp. 105–136.
- M. Fourmigué, in *Halogen Bonding: Fundamentals and Applications*, ed. P. Metrangolo and G. Resnati, Springer Berlin Heidelberg, Berlin, Heidelberg, 2008, pp. 181–207.
- T. M. Beale, M. G. Chudzinski, M. G. Sarwar and M. S. Taylor, *Chem. Soc. Rev.*, 2013, **42**, 1667–1680.
- M. Erdélyi, *Chem. Soc. Rev.*, 2012, **41**, 3547–3557.
- A.-C. C. Carlsson, A. X. Veiga and M. Erdélyi, in *Halogen Bonding II*, ed. P. Metrangolo and G. Resnati, Springer International Publishing, Cham, 2014, vol. 359, pp. 49–76.
- Y. Zhao, Y. Cotellet, N. Sakai and S. Matile, *J. Am. Chem. Soc.*, 2016, **138**, 4270–4277.
- L. C. Gilday, S. W. Robinson, T. A. Barendt, M. J. Langton, B. R. Mullaney and P. D. Beer, *Chem. Rev.*, 2015, **115**, 7118–7195.
- G. R. Desiraju, P. S. Ho, L. Kloo, A. C. Legon, R. Marquardt, P. Metrangolo, P. Politzer, G. Resnati and K. Rissanen, *Pure Appl. Chem.*, 2013, **85**, 1711–1713.
- O. Hassel, *Science*, 1970, **170**, 497–502.
- J. P. M. Lommerse, A. J. Stone, R. Taylor and F. H. Allen, *J. Am. Chem. Soc.*, 1996, **118**, 3108–3116.
- J. P. M. Lommerse, A. J. Stone, R. Taylor and F. H. Allen, *J. Am. Chem. Soc.*, 1996, **118**, 3108–3116.
- G. A. Landrum, N. Goldberg and R. Hoffmann, *J. Chem. Soc., Dalton Trans.*, 1997, 3605–3613.
- J.-M. Dumas, M. Gmel and M. Guerin, in *Halides, Pseudo-Halides and Azides (1983)*, ed. S. Patai and Z. Rappoport, John Wiley & Sons, Ltd., 1983, pp. 985–1020.
- A. C. Legon, *Angew. Chem., Int. Ed.*, 1999, **38**, 2686–2714.
- Z. P. Shields, J. S. Murray and P. Politzer, *Int. J. Quantum Chem.*, 2010, **110**, 2823–2832.
- C. C. Robertson, R. N. Perutz, L. Brammer and C. A. Hunter, *Chem. Sci.*, 2014, **5**, 4179–4183.
- M. Novák, C. Foroutan-Nejad and R. Marek, *Phys. Chem. Chem. Phys.*, 2015, **17**, 6440–6450.
- T. Clark, M. Hennemann, J. S. Murray and P. Politzer, *J. Mol. Model.*, 2007, **13**, 291–296.
- M. T. Messina, P. Metrangolo, W. Panzeri, E. Ragg and G. Resnati, *Tetrahedron Lett.*, 1998, **39**, 9069–9072.
- K. Eskandari and M. Lesani, *Chem. – Eur. J.*, 2015, **21**, 4739–4746.
- L. P. Wolters, P. Schyman, M. J. Pavan, W. L. Jorgensen, F. M. Bickelhaupt and S. Kozuch, *Wiley Interdiscip. Rev.: Comput. Mol. Sci.*, 2014, **4**, 523–540.
- For a review of XB...anion interactions in the solid state, see: G. Cavallo, P. Metrangolo, T. Pilati, G. Resnati, M. Sansotera and G. Terraneo, *Chem. Soc. Rev.*, 2010, **39**, 3772–3783.
- For an additional review of XB...anion interactions in the solid state, see: P. Metrangolo, T. Pilati, G. Terraneo, S. Biella and G. Resnati, *CrystEngComm*, 2009, **11**, 1187–1196.
- A. Mele, P. Metrangolo, H. Neukirch, T. Pilati and G. Resnati, *J. Am. Chem. Soc.*, 2005, **127**, 14972–14973.
- M. G. Sarwar, B. Dragisic, S. Sagoo and M. S. Taylor, *Angew. Chem., Int. Ed.*, 2010, **49**, 1674–1677.
- E. Dimitrijević, O. Kvak and M. S. Taylor, *Chem. Commun.*, 2010, **46**, 9025–9027.
- M. G. Sarwar, B. Dragisic, E. Dimitrijević and M. S. Taylor, *Chem. – Eur. J.*, 2013, **19**, 2050–2058.
- For an example, see: A. H. McKie, S. Friedland and F. Hof, *Org. Lett.*, 2008, **10**, 4653–4655.
- For a review of tripodal HB anion receptors, see: S. K. Dey, A. Basu, R. Chutia and G. Das, *RSC Adv.*, 2016, **6**, 26568–26589.
- S. H. Jungbauer, S. Schindler, E. Herdtweck, S. Keller and S. M. Huber, *Chem. – Eur. J.*, 2015, **21**, 13625–13636.
- M. G. Chudzinski, C. A. McClary and M. S. Taylor, *J. Am. Chem. Soc.*, 2011, **133**, 10559–10567.
- Z.-X. Liu, Y. Sun, Y. Feng, H. Chen, Y.-M. He and Q.-H. Fan, *Chem. Commun.*, 2016, **52**, 2269–2272.
- A. Vargasjentsch, D. Emery, J. Mareda, P. Metrangolo, G. Resnati and S. Matile, *Angew. Chem., Int. Ed.*, 2011, **50**, 11675–11678.
- A. V. Jentsch, D. Emery, J. Mareda, S. K. Nayak, P. Metrangolo, G. Resnati, N. Sakai and S. Matile, *Nat. Commun.*, 2012, **3**, 905.

- 46 A. Vargas Jentzsch and S. Matile, *J. Am. Chem. Soc.*, 2013, **135**, 5302–5303.
- 47 C. J. Serpell, J. Cookson, A. L. Thompson and P. D. Beer, *Chem. Sci.*, 2011, **2**, 494–500.
- 48 G. T. Spence, C. J. Serpell, J. Sardinha, P. J. Costa, V. Félix and P. D. Beer, *Chem. – Eur. J.*, 2011, **17**, 12955–12966.
- 49 J. Yoon, S. K. Kim, N. J. Singh and K. S. Kim, *Chem. Soc. Rev.*, 2006, **35**, 355.
- 50 Z. Xu, S. K. Kim and J. Yoon, *Chem. Soc. Rev.*, 2010, **39**, 1457.
- 51 C. J. Serpell, N. L. Kilah, P. J. Costa, V. Félix and P. D. Beer, *Angew. Chem., Int. Ed.*, 2010, **49**, 5322–5326.
- 52 A. Caballero, S. Bennett, C. J. Serpell and P. D. Beer, *CrystEngComm*, 2013, **15**, 3076–3081.
- 53 M. Cametti, K. Raatikainen, P. Metrangolo, T. Pilati, G. Terraneo and G. Resnati, *Org. Biomol. Chem.*, 2012, **10**, 1329–1333.
- 54 S. Zhang, Z. Chen, Y. Lu, Z. Xu, W. Wu, W. Zhu, C. Peng and H. Liu, *RSC Adv.*, 2015, **5**, 74284–74294.
- 55 A. Bondi, *J. Phys. Chem.*, 1964, **68**, 441–451.
- 56 A. Caballero, N. G. White and P. D. Beer, *Angew. Chem., Int. Ed.*, 2011, **50**, 1845–1848.
- 57 F. Zapata, A. Caballero, N. G. White, T. D. W. Claridge, P. J. Costa, V. Félix and P. D. Beer, *J. Am. Chem. Soc.*, 2012, **134**, 11533–11541.
- 58 A. Caballero, N. G. White and P. D. Beer, *CrystEngComm*, 2014, **16**, 3694–3698.
- 59 N. G. White, A. Caballero and P. D. Beer, *CrystEngComm*, 2014, **16**, 3722–3729.
- 60 N. L. Kilah, M. D. Wise and P. D. Beer, *Cryst. Growth Des.*, 2011, **11**, 4565–4571.
- 61 S. Chakraborty, R. Dutta and P. Ghosh, *Chem. Commun.*, 2015, **51**, 14793–14796.
- 62 N. B. Wageling, G. F. Neuhaus, A. M. Rose, D. A. Decato and O. B. Berryman, *Supramol. Chem.*, 2015, 1–8.
- 63 S. H. Jungbauer and S. M. Huber, *J. Am. Chem. Soc.*, 2015, **137**, 12110–12120.
- 64 Y. Hua and A. H. Flood, *Chem. Soc. Rev.*, 2010, **39**, 1262.
- 65 A. Kumar and P. S. Pandey, *Org. Lett.*, 2008, **10**, 165–168.
- 66 N. G. White, S. Carvalho, V. Félix and P. D. Beer, *Org. Biomol. Chem.*, 2012, **10**, 6951.
- 67 B. Nepal and S. Scheiner, *Chem. – Eur. J.*, 2015, **21**, 13330–13335.
- 68 R. Tepper, B. Schulze, M. Jäger, C. Friebe, D. H. Scharf, H. Görls and U. S. Schubert, *J. Org. Chem.*, 2015, **80**, 3139–3150.
- 69 B. Nepal and S. Scheiner, *J. Phys. Chem. A*, 2015, **119**, 13064–13073.
- 70 R. Tepper, B. Schulze, H. Görls, P. Bellstedt, M. Jäger and U. S. Schubert, *Org. Lett.*, 2015, **17**, 5740–5743.
- 71 T. K. Mole, W. E. Arter, I. Marques, V. Félix and P. D. Beer, *J. Organomet. Chem.*, 2015, **792**, 206–210.
- 72 L. C. Gilday, N. G. White and P. D. Beer, *Dalton Trans.*, 2013, **42**, 15766.
- 73 S. Kubik, *Chem. Soc. Rev.*, 2010, **39**, 3648–3663.
- 74 M. J. Langton, C. J. Serpell and P. D. Beer, *Angew. Chem., Int. Ed.*, 2016, **55**, 1974–1987.
- 75 K. I. Assaf, M. S. Ural, F. Pan, T. Georgiev, S. Simova, K. Rissanen, D. Gabel and W. M. Nau, *Angew. Chem., Int. Ed.*, 2015, **54**, 6852–6856.
- 76 P. W. Snyder, M. R. Lockett, D. T. Moustakas and G. M. Whitesides, *Eur. Phys. J.: Spec. Top.*, 2013, **223**, 853–891.
- 77 F. Biedermann, W. M. Nau and H.-J. Schneider, *Angew. Chem., Int. Ed.*, 2014, **53**, 11158–11171.
- 78 J. Y. C. Lim and P. D. Beer, *Chem. Commun.*, 2015, **51**, 3686–3688.
- 79 F. Zapata, A. Caballero, P. Molina, I. Alkorta and J. Elguero, *J. Org. Chem.*, 2014, **79**, 6959–6969.
- 80 J. Y. C. Lim, I. Marques, L. Ferreira, V. Félix and P. D. Beer, *Chem. Commun.*, 2016, **52**, 5527–5530.
- 81 J. Y. C. Lim, M. J. Cunningham, J. J. Davis and P. D. Beer, *Chem. Commun.*, 2015, **51**, 14640–14643.
- 82 G. T. Spence and P. D. Beer, *Acc. Chem. Res.*, 2013, **46**, 571–586.
- 83 M. J. Langton and P. D. Beer, *Acc. Chem. Res.*, 2014, **47**, 1935–1949.
- 84 N. L. Kilah, M. D. Wise, C. J. Serpell, A. L. Thompson, N. G. White, K. E. Christensen and P. D. Beer, *J. Am. Chem. Soc.*, 2010, **132**, 11893–11895.
- 85 J. M. Mercurio, R. C. Knighton, J. Cookson and P. D. Beer, *Chem. – Eur. J.*, 2014, **20**, 11740–11749.
- 86 S. P. Cornes, C. H. Davies, D. Blyghton, M. R. Sambrook and P. D. Beer, *Org. Biomol. Chem.*, 2015, **13**, 2582–2587.
- 87 L. C. Gilday and P. D. Beer, *Chem. – Eur. J.*, 2014, **20**, 8379–8385.
- 88 B. R. Mullaney, B. E. Partridge and P. D. Beer, *Chem. – Eur. J.*, 2015, **21**, 1660–1665.
- 89 S. W. Robinson, C. L. Mustoe, N. G. White, A. Brown, A. L. Thompson, P. Kennepohl and P. D. Beer, *J. Am. Chem. Soc.*, 2015, **137**, 499–507.
- 90 M. J. Langton, S. W. Robinson, I. Marques, V. Félix and P. D. Beer, *Nat. Chem.*, 2014, **6**, 1039–1043.
- 91 L. M. Hancock and P. D. Beer, *Chem. – Eur. J.*, 2009, **15**, 42–44.
- 92 M. J. Langton, I. Marques, S. W. Robinson, V. Félix and P. D. Beer, *Chem. – Eur. J.*, 2016, **22**, 185–192.
- 93 A. Caballero, F. Zapata, N. G. White, P. J. Costa, V. Félix and P. D. Beer, *Angew. Chem., Int. Ed.*, 2012, **51**, 1876–1880.
- 94 B. R. Mullaney, A. L. Thompson and P. D. Beer, *Angew. Chem., Int. Ed.*, 2014, **53**, 11458–11462.
- 95 M. J. Langton, Y. Xiong and P. D. Beer, *Chem. – Eur. J.*, 2015, **21**, 18910–18914.
- 96 A. Bauzá, T. J. Mooibroek and A. Frontera, *ChemPhysChem*, 2015, **16**, 2496–2517.
- 97 P. Politzer, K. E. Riley, F. A. Bulat and J. S. Murray, *Comput. Theor. Chem.*, 2012, **998**, 2–8.
- 98 P. Politzer and J. S. Murray, *ChemPhysChem*, 2013, **14**, 278–294.
- 99 S. Alvarez, *Dalton Trans.*, 2013, **42**, 8617.